Widespread, depth-dependent microstructural damage in the cortex of children with drug resistant focal epilepsy: A quantitative T1 and T2 mapping study

Author names and affiliations:

Chiara Casella[1*], Katy Vecchiato[1,2*], Daniel Cromb[1], Yourong Guo[2], Anderson M. Winkler[3], Emer Hughes[1], Louise Dillon[1], Elaine Green[1], Kathleen Colford[1], Alexia Egloff[1], Ata Siddiqui[4], Anthony Price[1], Lucilio Cordero Grande[5,6], Tobias C. Wood[7], Shaihan Malik[5], Rui Pedro A.G. Teixeira[5], David W. Carmichael[5], Jonathan O'Muircheartaigh[1,2,8]

[1]Centre for the Developing Brain, School of Biomedical Engineering and Imaging Sciences, King's College London, London, UK; [2]Department for Forensic and Neurodevelopmental Sciences, Institute of Psychiatry, Psychology and Neuroscience, King's College London, London, UK; [3]Department of Human Genetics, University of Texas Rio Grande Valley, Brownsville, Texas, United States; [4]Department of Radiology, Guy's and Saint Thomas' Hospitals NHS Trust, London, UK; [5]Department of Biomedical Engineering, King's College, London, UK; [6]Biomedical Image Technologies, ETSI Telecomunicación, Universidad Politécnica de Madrid & CIBER-BBN, ISCIII, Madrid, Spain; [7]Department of Neuroimaging, King's College, London, UK; [8]MRC Centre for Neurodevelopmental Disorders, UK.

*These authors share first authorship

Corresponding author:

Chiara Casella: chiara.casella@kcl.ac.uk

Abstract

Our current understanding of focal epilepsy is evolving as increasing evidence suggests that tissue abnormalities may extend beyond the focus. In adults, widespread structural changes remote from the putative epileptic focus have been demonstrated with MRI, predominantly using morphological markers. However, the underlying pathophysiology of these changes is unclear, and it is not known whether these result from ongoing disease processes or treatment-related side-effects, or whether they emerge earlier. Few studies have focused on children, who typically have shorter disease duration. Fewer still have utilised quantitative MRI, which may provide a more sensitive and interpretable measure of tissue microstructural changes.

In this study, we aimed to determine if there were common spatial modes of changes in cortical architecture in children with drug-resistant focal epilepsy, and secondarily if changes were related to disease severity. To assess cortical microstructure, quantitative T1 and T2 relaxometry (qT1 and qT2) was measured in 89 children - 43 with drug-resistant focal epilepsy [age-range=4-18 years] and 46 healthy controls [age-range=2-18 years]. We assessed depth-dependent qT1 and qT2 values across the cortex, as well as their gradient of change across cortical depths. As a post-hoc analysis, we determined whether global changes seen in group analyses were driven by focal pathologies in individual patients. Finally, we trained a classifier using qT1 and qT2 gradient maps from patients with radiologically-defined abnormalities (MRI-positive) and healthy controls, and tested if this could classify patients without reported radiological abnormalities (MRI-negative).

We detected depth-dependent qT1 and qT2 increases in widespread cortical areas, likely representing loss of structure such as altered cortical stratification, gliosis, myelin and iron alterations, oedema-associated increases in free-water, or a combination of these. Changes did not correlate with disease severity measures, suggesting they may appear during cerebral development and represent antecedent neurobiological alterations. Using a classifier trained with MRI-positive patients and controls, sensitivity was 62% at 100% specificity on held-out MRI-negative patients and controls.

Our findings suggest the presence of a potential imaging endophenotype of focal epilepsy, detectable irrespective of radiologically-identified abnormalities, and possibly evident at a pre-symptomatic disease stage.

Keywords:
Paediatric focal epilepsy, qMRI, relaxometry, cortical microstructure, FCD

1. Introduction

Subtle and widespread structural abnormalities have been demonstrated in focal epilepsy in cortical areas remote from the putative epileptic focus (R. S. Liu et al., 2003; Sisodiya et al., 1995). For example, multifocal grey matter (GM) volume changes have been reported in patients with malformations of cortical development (Woermann et al., 1999), and 41% of patients with chronic epilepsy show generalized cortical volume loss (R. S. Liu et al., 2003). These factors, together with incomplete resection, could contribute to why approximately 30% of patients are not seizure-free after surgery (Fauser et al., 2004). Though such cortical changes may be attributable to the adverse effects of medication (De Marcos et al., 2003; Latour et al., 2004), and ongoing and cumulative disease processes (Adler et al., 2018; Donaire et al., 2006), it is possible that such alterations cannot be ascribed to the downstream effects of epilepsy, such as seizure reoccurrence, and are instead linked to disease aetiology, thus representing a predisposing factor to the development of epilepsy (Sisodiya et al., 1995).

Most previous MRI studies in epilepsy have quantified structural morphological changes (Ahmad et al., 2020), including alterations in volume, surface area, and cortical thickness. However, despite providing useful information, morphological markers such as the ones above likely reflect the combination of several biological events, often provide redundant information (Winkler et al., 2018), and do not offer insight into the microstructural abnormalities underlying such changes. However, MRI also affords quantitative metrics which describe tissue microstructure, composition, and pathological processes. Quantitative MRI (qMRI) techniques such as longitudinal (T1) and transverse (T2) relaxation (qT1 and qT2) are sensitive to tissue structure and biophysical properties at the micrometre scale (Adler et al., 2017) and allow the in vivo assessment of inconspicuous changes in cortical tissue properties, such as myelin and iron abnormalities or alterations in free-water content (Cercignani et al., 2018).

Previous research has mapped the distribution of neocortical and hippocampal qT1 in adult patients with drug-resistant temporal lobe epilepsy (TLE) and healthy controls, revealing T1 increases in ipsilateral temporal and frontal limbic cortices, with more marked effects in upper cortical levels that taper off towards the GM/WM boundary. Increases were particularly marked in patients with early disease onset (Bernhardt et al., 2018). Additionally, Ahmad et al (2020), used qT2 relaxometry and surface-based analysis techniques to investigate normal-appearing cortical tissue in adult epilepsy patients with FCDs. Widespread cortical T2 increases in frontal, parietal, and some temporal regions were observed in the patient group, suggesting effects of the disease in cortical regions beyond FCD areas.

In the present study, we assessed whether such cortical microstructure changes can also be observed in children with drug resistant focal epilepsy. Crucially, because of shorter disease-duration, the assessment of children with epilepsy enables a deeper insight into whether cortical alterations previously reported in adults (Ahmad et al., 2020; Bernhardt et al., 2018; Caciagli et al., 2017; R. S. Liu et al., 2003; Woermann et al., 1999) may represent

antecedent neurobiological alterations (Widjaja et al., 2012), and possibly constitute a predisposing factor to disease development (Sisodiya et al., 1995).

Specifically, we assessed surface-based qT1 and qT2 values at increasing cortical depths (Glasser et al., 2013), as well as their gradient of change as an index of microstructural organization. We expected to detect, focal, rather than global, cortical abnormalities, because of shorter disease-duration (Bernhardt et al., 2018). The relationship of qT1 and qT2 changes to clinical parameters including age of onset, disease duration and number of seizures per year was also assessed. As a post-hoc analysis, based on previous evidence that quantitative diffusion and susceptibility imaging can detect cortical signatures of malformations of cortical development (Lorio et al., 2020, 2021), we assessed whether any changes seen in group differences were specific to (and therefore driven by) the focal cortical lesions of individual patients.

Finally, as exploratory analysis, we also evaluated the potential of qMRI to identify an imaging endophenotype of children at risk of focal epilepsy, detectable with or without radiologically-detected abnormalities being present. For this purpose, we trained a random forest classifier using whole-brain qT1 and qT2 cortical gradient maps from MRI-positive patients and healthy controls, and tested if this could classify MRI-negative patients and controls held out from the training phase.

2. Materials and methods

2.1. Subjects:

96 children were recruited for the present study (ethics ref. 18/LO/1766), 89 of which were included in the analysis - 43 with drug resistant focal epilepsy [age range: 4-18, mean = 12yrs, 22 female], and 46 healthy controls [age range: 2-18, mean = 11.5yrs, 27 female]. Of the 7 participants excluded from the analysis, 4 presented incidental findings and 3 had missing data. There was no significant difference in age between patients and controls assessed in the study (p=0.68).

Participants were recruited prospectively, and ethical approval was granted by the Health Research Authority (HRA) and Health and Care Research Wales (HCRW). Exclusion criteria were age younger than 6 months or older than 18 years, major neurologic conditions unrelated to epilepsy, and contraindications for 3T MR imaging.

Eligible patients were recruited through the paediatric neurology outpatient clinics at the Evelina London Children Hospital, King's College Hospital and Great Ormond Street Hospital, while children without epilepsy were recruited from existing volunteer databases, mainstream schools, and from the King's College London recruiting webpage.

For participants under 16 years of age, written signed consent was obtained from the parents (or the person with legal parental responsibility) prior to any data collection. Patients aged 5 to 15 were given the choice of signing an assent form. Adolescents 16 or over provided their own written consent to participate.

In patients, diagnosis and lateralization of the seizure focus were determined by a comprehensive evaluation including detailed history, neurological examination, review of medical records, video-EEG recordings, and clinical MRI evaluation. These revealed that, amongst the patients assessed, the majority had temporal involvement, followed by frontal, occipital, frontal/temporal, and parietal (Table 1).

Table 1. Descriptive demographics of the study sample.

Characteristics	Healthy Control Participants	Patients with Epilepsy	Total
Number	46	43	89
Age at scan (years)			
Mean + SD	11.54 ± 3.96	12 ± 3.56	11.85 ± 3.76
1 - 5	3	1	4
6 -10	18	14	32
11 - 15	17	20	37
16 - 18	8	8	16
Sex			
Male	19	21	40
Female	27	22	49

Focus laterality (hemisphere)			
Left	-	25	
Right	-	17	
Unknown		1	
Focus area (ratio/percentage)			
Frontal	-	14/43 (33%)	
Temporal	-	22/43 (51%)	
Frontal & Temporal	-	2/43 (4.5%)	
Occipital	-	3/43 (7%)	
Parietal	-	2/43 (4.5%)	
Age of onset			
Mean + SD	-	6.95 ± 3.01	
Disease duration			
Mean + SD	-	4.85 ± 3.16	
Number of seizures per year			
Mean + SD	-	173.46 ± 288.08	

2.2. Image Acquisition

Children were scanned without sedation on a 3T Achieva-TX (Philips Healthcare) using a 32-channel head coil. They were asked to stay still during scanning while watching a movie. The protocol included: a 3D T1-weighted MPRAGE [TR = 7.7ms, TE = 3.6ms, flip angle = 8°, TI = 900ms, echo-train length = 154 and acquisition time = 286s]; a T2-weighted FLAIR [TR = 5000ms, TE = 422ms, TI = 1800ms, echo-train length = 182, acquisition time = 510s]; a joint system relaxometry (JSR) acquisition (Teixeira et al., 2018), consisting of two SPGR (flip angle = 2.2° and 12.5°, TR = 6.2ms) and three bSSFP (with a 12° flip angle and a 180° phase increment, 49° flip angle and a 0° phase increment and 49° flip angle and a 180° phase increment respectively; all had a TR of 6ms). Parallel imaging acceleration (SENSE) of 1.4 was used along both phase-encoding directions. The field of view was 240 × 188 × 240mm, and the resolution was 1 mm isotropic for all images.

2.3. Motion Tolerance

All scans were acquired using the DISORDER scheme, which has demonstrated improved tolerance against motion by guaranteeing that the acquisition of every shot contains a series of samples distributed incoherently throughout k-space (Cordero-Grande et al., 2020; Vecchiato et al., 2021). With this modified sampling order, motion estimation and image reconstruction can be effectively performed jointly using a parallel k-space model in the presence of rigid motion. Starting from a standard reconstruction assuming no motion, a

first approximation of the motion parameters for each shot is obtained by maximizing the likelihood of the k-space measures for current reconstructed volume. Then a new volume is reconstructed with current motion parameters, and the method alternates between motion estimation and reconstruction until convergence. Thus, motion correction is entirely performed as part of the image reconstruction from k-space; an in-depth description of the reconstruction algorithm has been described previously (Cordero-Grande et al., 2016; Cordero-Grande et al., 2020).

2.4. Image Analysis (Figure 1):

Surface reconstruction: FLAIR and MPRAGE images were co-registered and jointly analysed with the Human Connectome Project structural pipeline (Glasser et al., 2013) to reconstruct WM/GM and pial surfaces. These surfaces were used to compute equi-volume cortical surface depths by sampling the surface vertices in steps of 20% of cortical volume (0%: WM/GM boundary, 100%: pial surface) across the entire cortex.

T1 and T2 surface mapping: JSR (Teixeira et al., 2018) fits were performed within the QUIT toolbox (Wood, 2018), providing 3D qT1 and qT2 relaxation time maps. qT1 and qT2 images were rigidly co-registered to the FLAIR and MPRAGE volume, smoothed ($\sigma = 0.4$) and projected to each cortical depth.

Between-group differences in cortical T1 and T2: Group-wise alterations at 20%, 40%, 60% and 80% cortical distance from the GM/WM border were tested. Additionally, vertex-wise qT1 and qT2 values at 20% distance were subtracted from those at 80% distance, and group differences in the gradient of change were tested, as an index of intracortical organization. Finally, associations between qT1 and qT2 changes in patients and age of disease onset, disease duration and number of seizures per year were assessed. Because of skewness in the data, the number of seizures per year data were log-transformed before assessing correlations. All analyses were run using permutation analysis of linear models (PALM) (Winkler et al., 2016), which allows inference using permutation methods.

All the above analyses were then repeated by splitting patients with temporal focus (N = 22) and patients with frontal focus (N = 14) into two sub-groups, to understand whether the focus area has a significant impact on the observed changes. For this step of the analysis, we excluded patients with occipital (N = 3) parietal (N = 2) focus, because of low numbers, as well as those patients who presented frontal and temporal focus (N = 2).

Finally, we repeated the above analysis by splitting patients into two other sub-groups according to their focus laterality, to understand whether the latter affected the examined changes. One patient was excluded from this analysis because of uncertain hemispheric focus.

As a first step, for all analyses we tested for an interaction between age and group, but this was not significant. Age as well as sex were thus regarded as covariates of no interest in the final analyses. Cortical thickness was also controlled for in the analyses, because of evidence that this feature is altered in epilepsy (Galovic et al., 2020; R. S. Liu et al., 2003). Finally, differences in cortical curvature have been shown to systematically affect the laminar and myeloarchitecture of the cortex (Annese et al., 2004), so that strong correlations between

local curvature and R1 (1/T1) can be observed. Therefore, in our analyses, we also controlled for individual differences in vertex-wise cortical curvature. In all analyses, a conservative single family-wise error correction rate was applied across MRI modalities (i.e. qT1 and qT2) and statistical contrasts. In all analyses, threshold-free cluster enhancement (TFCE) was employed as a test statistic (Smith & Nichols, 2009), and permutations in PALM used the method of Draper-Stoneman (Winkler et al., 2014),which ensures that spatial dependencies in the data are preserved for all permutations, given our modelling of vertexwise cortical thickness and curvature as nuisance.

Surface-based qMRI profiles of focal cortical dysplasias (FCDs) (Figure 2): To assess whether changes seen in group differences may have been driven by the focal lesions of individual patients, we performed a post-hoc examination of the qMRI profiles of lesions of 7 patients with confirmed FCDs. For this purpose, we first manually delineated lesion masks on the FLAIR images in each patient. We then mapped the lesion masks to each cortical depth in both patients and controls in the HCP standard surface space, which is made up of approximately 32,000 vertices (Glasser et al., 2013). Finally, we extracted the unpermuted residuals of qT1 and qT2 values at different cortical depths within the lesion area. These were computed as follows: Y-Z*g, where Z is the matrix with confounds (i.e. age, sex, thickness and curvature) and g are the estimated GLM regression coefficients from Y = X*b + Z*g.

This allowed computation of the z-score profile of each patient against controls, corrected for age and sex. Importantly, for this part of the analysis, we further extended the spatial sampling to 1mm below the GM/WM border.

Assessment of the diagnostic performance of surface-based 3T relaxometry supported through a Random Forest automatic classification algorithm: Using Scikit-learn (Pedregosa et al., 2011), a random forest algorithm (Breiman, 2001) was trained on the gradient maps of qT1 and qT2 unpermuted residuals of MRI-positive patients (N=21) and controls (N=31). Each subject's vertex-wise qT1 and qT2 residuals for left and right were concatenated and fed to the classifier (Figure 3). The model's performance was tested on gradient maps of qT1 and qT2 unpermuted residuals of MRI-negative patients (N=19) and controls (N=14) held-out from the training set. Area under the ROC Curve (AUC), accuracy, sensitivity, specificity and F1-scores were used to evaluate classification performance. A permutation-based p-value was calculated to assess the probability that the observed results could have been obtained by chance.

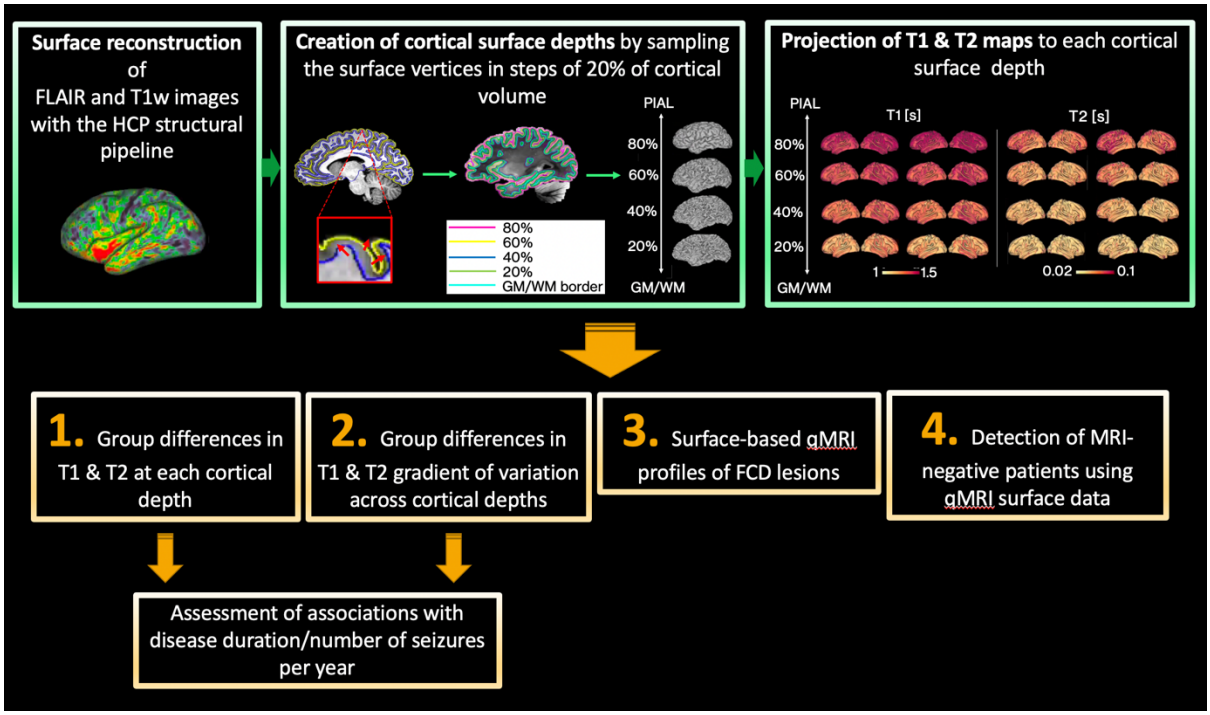

Figure 1. Diagram of data processing (green boxes) and analysis (orange boxes). *First, surface reconstruction was performed with the HCP structural pipeline (Glasser et al., 2013). Then, surface extraction was performed at a series of cortical depths and qT1 and qT2 maps were projected onto each depth. This allowed the assessment of group differences in: (1) qT1 and qT2 values at several depths from the pial surface; (2) qT1 and qT2 gradient of variation across cortical depths. Associations with disease duration and number of seizures per year were also explored. We also computed surface-based qMRI profiles of FCD lesions (3), and assessed whether cortical microstructure patterns learnt from MRI-positive patients could classify MRI-negative patients (4).*

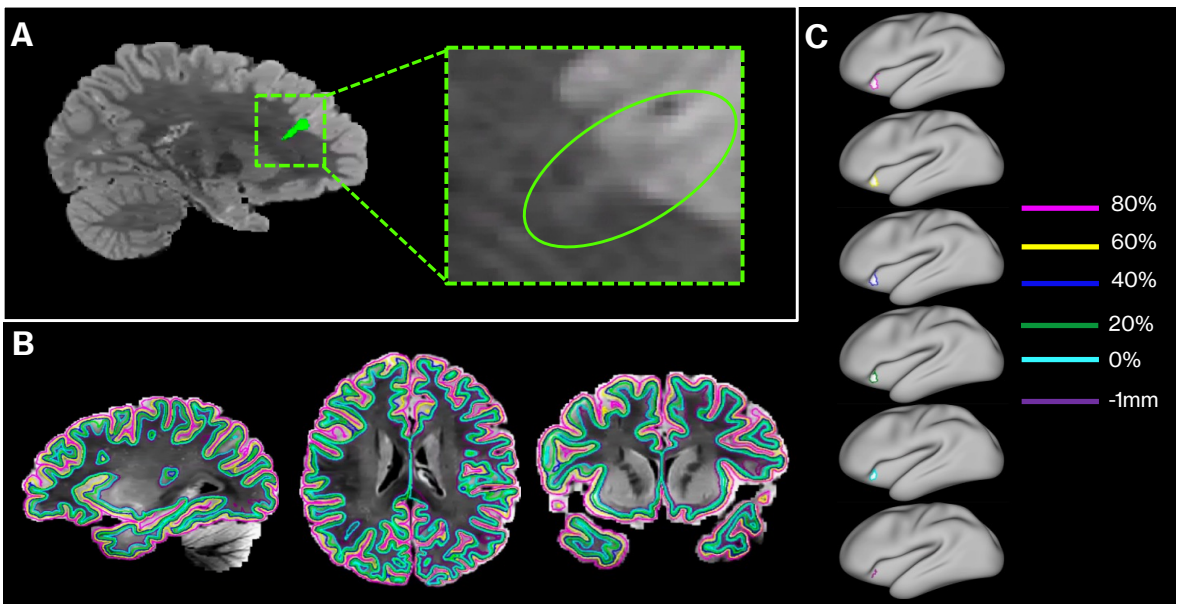

Figure 2. Workflow of the computation of surface-based qMRI profiles of FCD lesions. *(A) Lesion masks were delineated on the FLAIR images of each of the 7 patients with FCDs; (B) Surface extraction at increasing depths was performed on MPRAGE and FLAIR images; (C) The lesion masks were then mapped to each cortical depth in patients and controls in standard surface space.*

3. Results

3.1. Group differences in qT1 and qT2 at each depth from the GM/WM border

Figure 3 highlights the areas of significant group differences in qT1 and qT2 at each cortical depth. When comparing all patients against controls, we detected increased qT2 in patients in the outermost cortical depths (i.e. at 60% and 80% from the GM/WM border). Figure 5A displays subject-average qT1 and qT2 values grouped into patients and controls in areas where significant group differences were detected, at 80% distance from the GM/WM border.

When splitting patients into frontal versus temporal lobe focus, qT1 were detected at 80% distance from the GM/WM border in the left temporal lobe of TLE patients. Additionally, qT2 increases were detected at 60 and 80% distance from the GM/WM border in TLE patients, especially in the left hemisphere, which was the one affected in most of these patient subgroup. Though stronger effects could be detected in the temporal lobe, increases in qT2 also affected frontal, occipital and parietal lobes, especially at 80% distance. We detected no significant differences between frontal patients and controls, nor between the two patients' sub-groups.

After splitting the patient group into two sub-groups based on focus laterality, increases in qT2 at the 60% and 80% distance from the GM/WM border could be detected between patients with left-hemisphere focus and controls. Although the effects were stronger in the left hemisphere, increases in qT2 were spread across the two hemispheres. Additionally, increases in qT1 could be detected at 80% depth from the GM/WM border in patients with left-hemisphere focus. Though some small significant clusters could be observed in the right hemisphere, the majority of qT1 increases involved the left hemisphere, and were mostly concerning temporal and parietal lobes. No significant differences were detected between patients with right-hemisphere focus and controls, nor between the two patients' sub-groups.

With both analysis approaches, we did not detect any association between microstructure changes and clinical variables. However, there was a positive relationship between disease duration and age in patients (rho = 0.59, $p < 0.001$), potentially indicating the presence of collinearity, which in turn might have impacted our sensitivity to associations between microstructural changes and clinical variables.

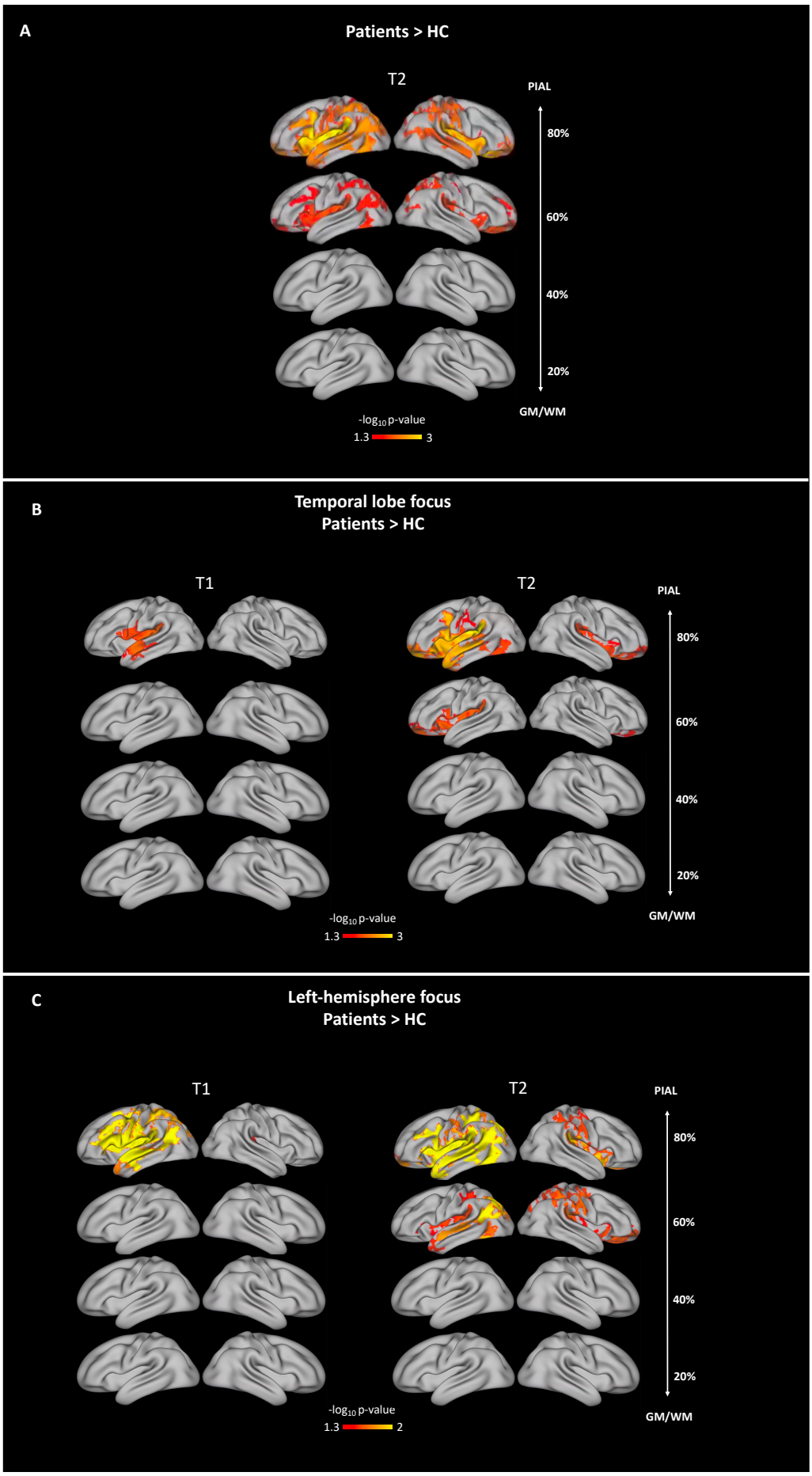
A
Patients > HC
T2
PIAL
80%
60%
40%
20%
GM/WM
-log10 p-value
1.3
3
B
Temporal lobe focus
Patients > HC
T1
T2
PIAL
80%
60%
40%
20%
GM/WM
-log10 p-value
1.3
3
C
Left-hemisphere focus
Patients > HC
T1
T2
PIAL
80%
60%
40%
20%
GM/WM
-log10 p-value
1.3
2

Figure 3 Group differences between patients and healthy controls (HC) in qT1 and qT2 at each depth from the GM/WM border. *(A) Widespread increases in qT2 at 60 and 80% distance from the WM/GM boundary were detected in patients. (B) When splitting patients into frontal versus temporal lobe focus, qT1 increases were detected in the left temporal lobe in TLE patients. Additionally, qT2 increases were detected at 60 and 80% distance from the GM/WM border in TLE patients, especially in the left hemisphere. Increases in qT2 affected frontal, occipital and parietal lobe as well as the temporal lobe, especially at 80% distance. When splitting patients into subgroups based on focus laterality, qT1 and qT2 increases were detected in the outermost cortical depths in patients with left hemispheric focus compared to healthy controls. While qT1 changes appear to mostly relate the left hemisphere, qT2 increases are more widespread in these patients, suggesting that these changes extend beyond the focal hemisphere.*

3.2. Group differences in qT1 and qT2 gradients as an index of intracortical organization

A "surface-out" gradient, driven from the WM/GM border, of increasing qT1 and qT2 values could be seen across the cortex in both patients and controls. Permutation tests revealed a significant difference between the two groups in cortical qT1 and qT2 gradients, indicating a steeper gradient of variation across cortical depths in the patient group, with increasingly higher qT1 and qT2 values in the outermost cortical depths across the two hemispheres (Figure 4). Figure 5B displays subject-average qT1 and qT2 gradient values grouped into patients and controls in areas where significant group differences were detected.

After splitting patients based on temporal versus frontal focus, we detected steeper variation of qT1 and qT2 values across cortical depths in patients with TLE. The changes concerned mostly the left hemisphere, which was the one affected in most TLE patients, and extended beyond the temporal lobe, affecting most of the cortex. We detected no significant differences between frontal patients and controls, nor between the two patients' sub-groups, and no significant associations with clinical variables.

Finally, when splitting patients based on focus laterality, we detected significantly steeper gradients in patients with left-hemisphere focus, again demonstrating increasingly higher qT1 and qT2 values in the outmost cortical depths. The effects were widespread and bilateral, however they were stronger in the left hemisphere. No significant differences between the two patients' sub-groups, and no significant associations with clinical variables, could be detected.

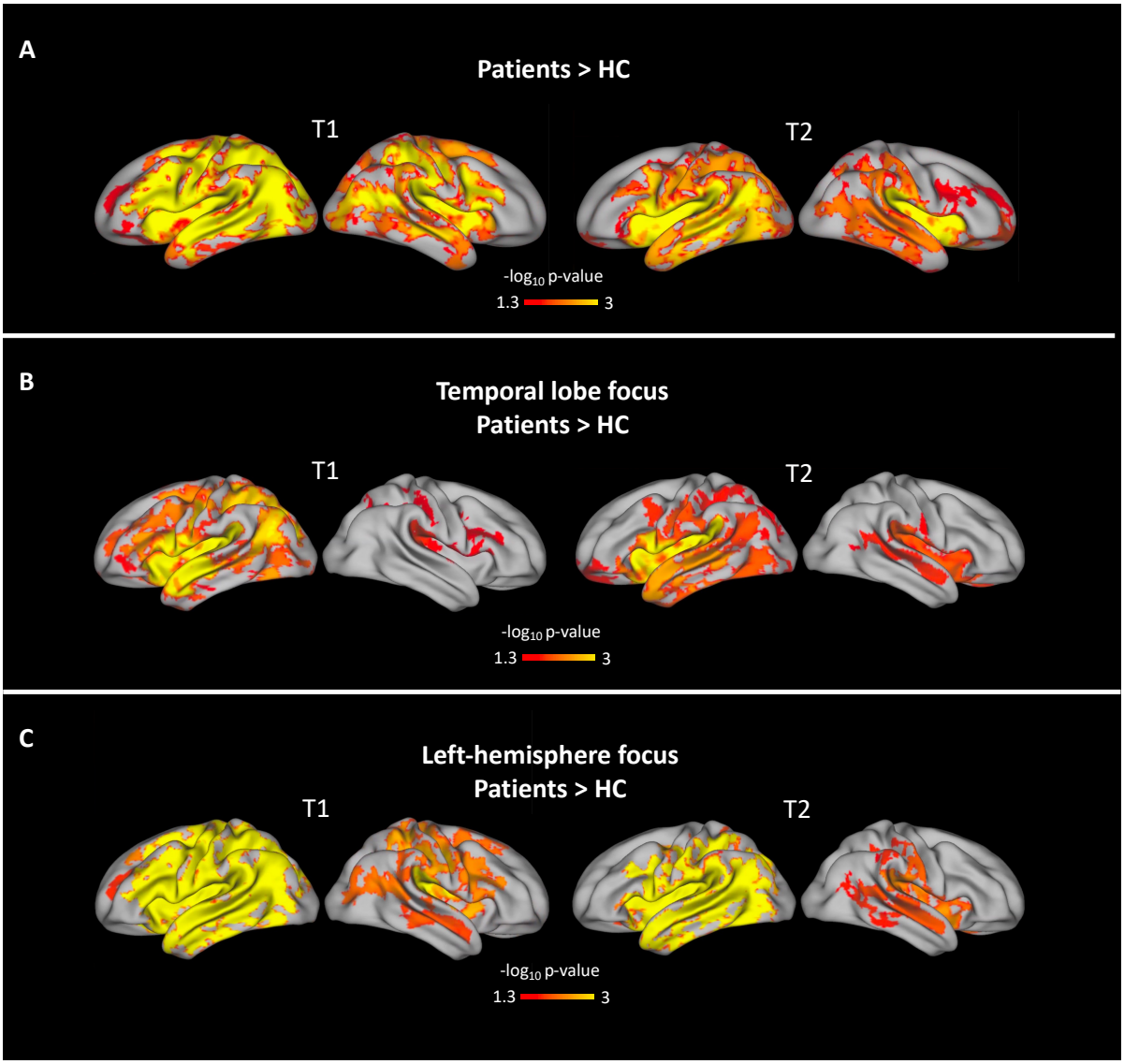

Figure 4. Group differences in qT1 and qT2 gradients as an index of intracortical organization. *(A) Group differences in the gradient of variation in qT1 and qT2: widespread steeper qT1 and qT2 variation was detected in patients, with increasingly higher values in the outermost cortical layers. (B) When splitting patients into subgroups based on temporal versus frontal lobe focus, widespread steeper qT1 and qT2 variation was detected in patients with temporal lobe focus. Such changes extended beyond temporal areas, especially in the left hemisphere, which was the hemisphere affected in most TLE patients. (C) When splitting patients into subgroups based on focus laterality, widespread steeper qT1 and qT2 variation was detected in patients with left hemisphere focus across both hemispheres, though the effect was stronger in the left hemisphere.*

A

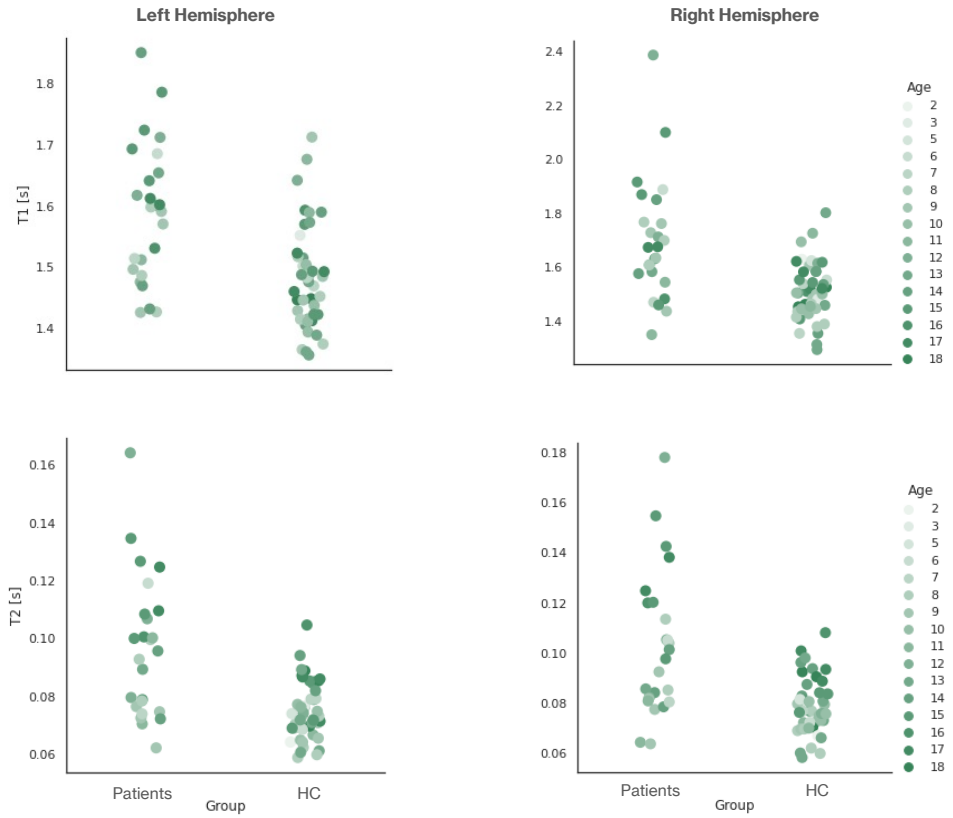
Left Hemisphere
Right Hemisphere
T1 [s]
T2 [s]
Age
2
3
5
6
7
8
9
10
11
12
13
14
15
16
17
18
Patients
HC
Group

B

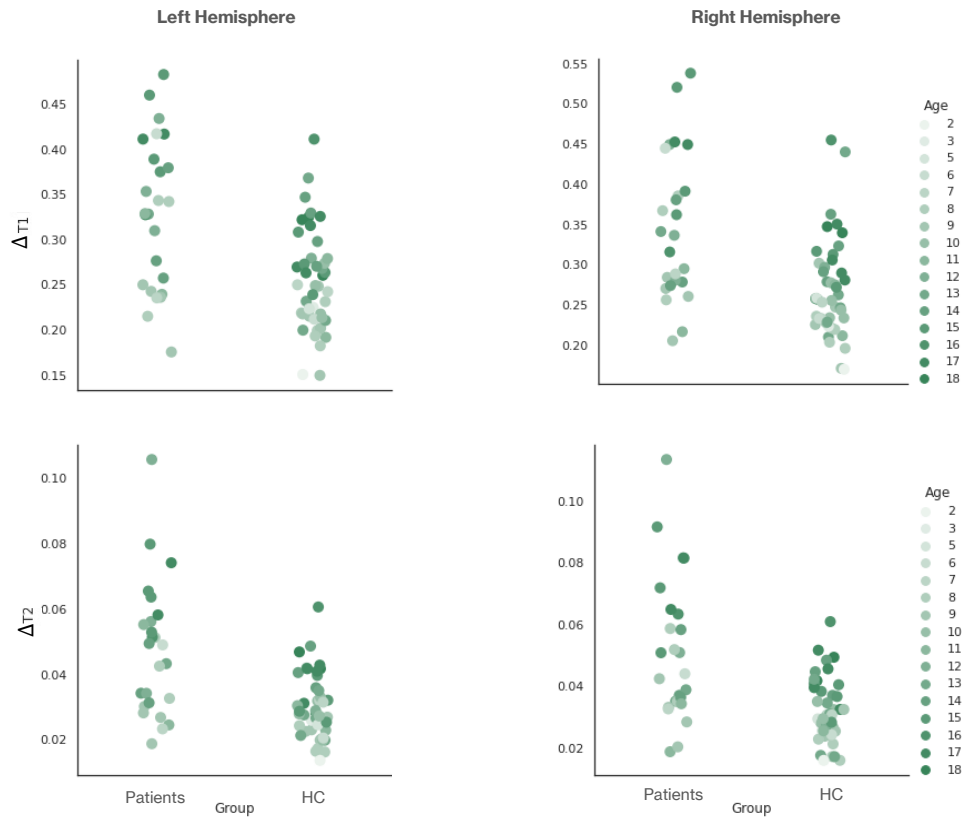
Left Hemisphere
Right Hemisphere
Δ T1
ΔT2
Age
2
3
5
6
7
8
9
10
11
12
13
14
15
16
17
18
Patients
HC
Group

Figure 5. Illustrative strip plot of average qT1 and qT2 values*. (A) Average qT1 and qT2 values are displayed for each subject across patients and healthy controls (HC) in areas where significant group differences were detected, at 80% distance from the GM/WM border. (B) Average qT1 and qT2 gradient values are displayed for each subject across patients and healthy controls (HC) in areas where significant group differences were detected.*

3.3. Surface-based qMRI profiles of FCD lesions

Figure 6 illustrates the surface maps of the focal cortical dysplasia (FCD) locations (A), as well as the z-score profiles of FCD lesions across the different cortical depths (B), for each of the patients assessed. The detected changes were heterogeneous between lesions, with no consistent pattern of change in qT1 or qT2, suggesting that spatial modes of qT1 and qT2 alterations are not driven by focal abnormalities (C).

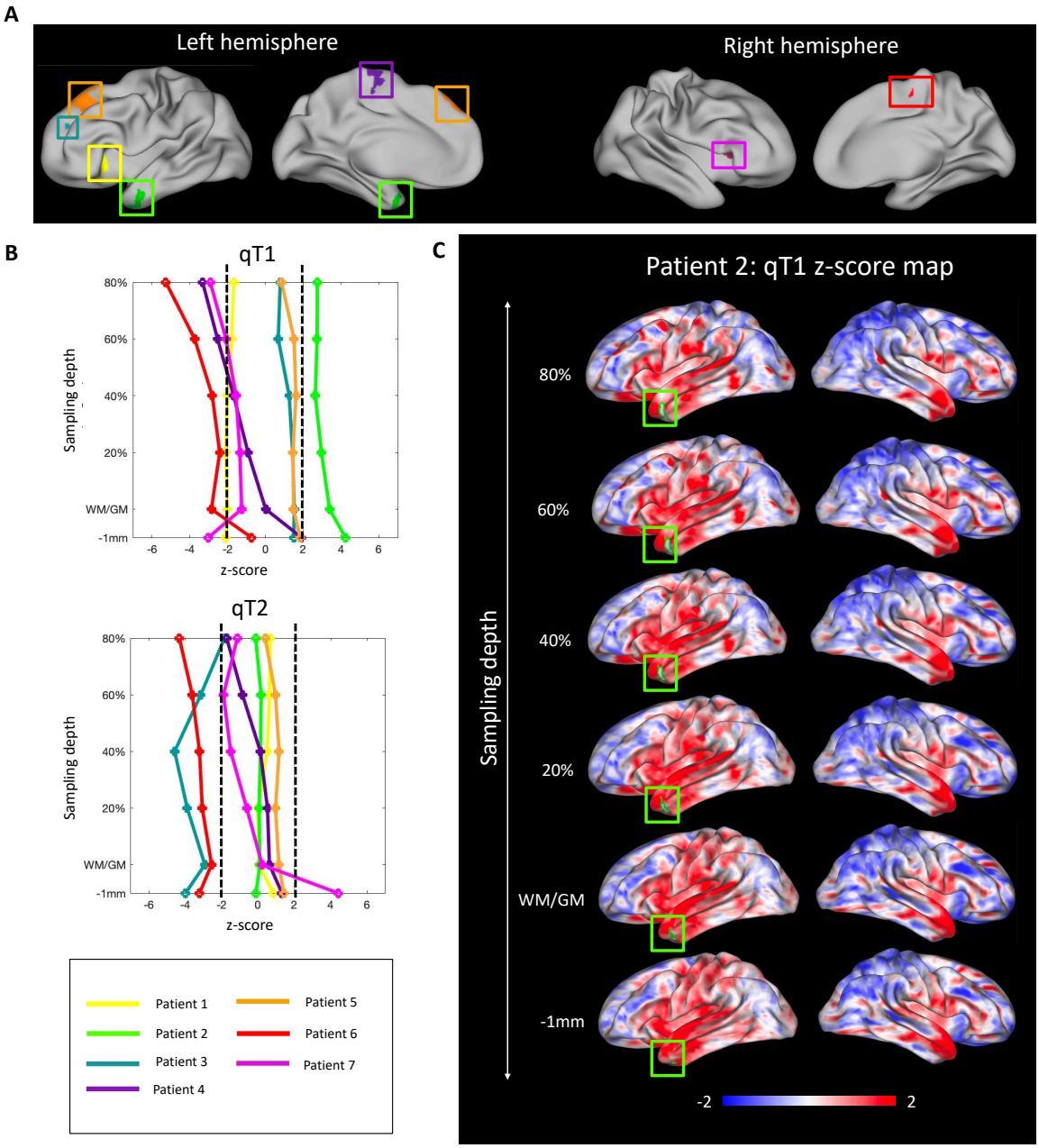

Figure 6. Spatial modes of qT1 and qT2 alterations are not driven by focal abnormalities. *(A) Surface maps of FCDs locations of all patients. Lateral and medial views are presented for both hemispheres. The FCDs were located in temporal, frontal and parietal areas. (B) qMRI z-score profiles of FCDs for qT1 (top) and qT2 (bottom). Here, each line represents the z-score deviation of one patient against all controls, across cortical depths. Any z-score greater than +2 or smaller than -2 (black dashed lines) represents a significant deviation from the control distribution. Detected changes were heterogeneous between lesions, with no consistent pattern of change across measures and patients. (C) qT1 z-scores map of a representative subject (Patient 2). A significant positive deviation from the control sample could be detected in qT1 for this patient within the FCD (B, top graph). Though high z-scores can be observed within the lesion, increases in qT1 extend beyond the lesion area, across cortical regions and hemispheres.*

3.4. Assessment of the diagnostic performance of surface-based 3T relaxometry supported through a Random Forest automatic classification algorithm (Figure 7):

On a classifier trained with MRI-positive patients and controls, we had a test AUC of 95%, accuracy of 82%, sensitivity of 62% at 100% specificity, and an F1 score of 75% on MRI-negative patients and controls that were not part of the training group. The potential for classification cannot be attributed to chance [p = 0.001].

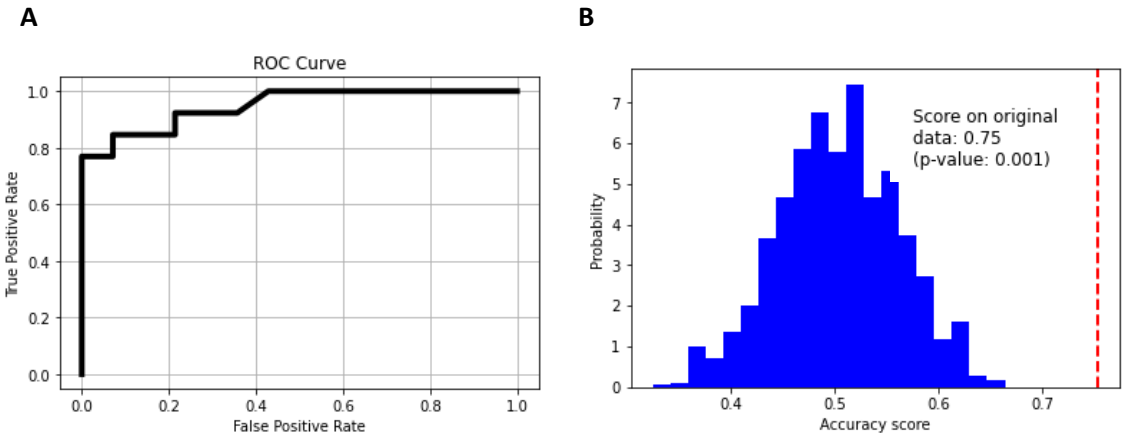

Figure 7. Random Forest Classifier performance. *(A) ROC Curve. (B)Histogram of the permutation scores (the null distribution). The red line indicates the score obtained by the classifier on the original data. The score is much better than that obtained by using permuted data and the p-value is significant.*

4. Discussion

Increasing evidence suggests that cortical abnormalities in focal epilepsy may exist across extended spatial regions. In this work, we assessed cortical changes in children with drug resistant focal epilepsy. Because of shorter disease-duration, the assessment of a paediatric sample enabled deeper insight into whether these alterations are the result of ongoing chronic disease-processes (Adler et al., 2018; Donaire et al., 2006) and treatment-related side-effects (De Marcos et al., 2003; Latour et al., 2004), or whether they emerge at an earlier disease-stage (Sisodiya et al., 1995; Widjaja et al., 2012). Crucially, the use of a multiparametric qMRI approach allowed to move beyond quantification of morphological markers, such as cortical thickness, GM density, or FLAIR intensity, and probe changes in cortical tissue microstructure, such as myelin and iron abnormalities or alterations in free-water content (Cercignani et al. 2018).

Overall, our findings indicate the presence of widespread, depth-mediated qT1 and qT2 increases in a heterogeneous sample of children with focal epilepsy. Additionally, they demonstrate significant alterations in patients' intracortical organization (Lorio et al., 2021), as shown by a "surface-out" gradient of increased qT1 and qT2 values driven from the WM/GM border in patients. Consistent with previous evidence (Ahmad et al., 2020; Bernhardt et al., 2018; Hattingen et al., 2018), the observed cortical changes were robust to potential confounders, including age-variation and differences in vertex-wise cortical thickness and curvature, suggesting that they represent a different underlying pathophysiological mechanism. Additionally, the detected alterations did not appear specific to, or driven by, the focal cortical lesions of patients, as demonstrated by the observed heterogeneity of qMRI profiles within the investigated FCDs. Importantly, in accord with previous studies (Ahmad et al., 2020; R. S. Liu et al., 2003), clinical parameters did not correlate with qT1 and T2 values across the cortex, implying that such microstructural alterations may be independent of ongoing disease processes. Interestingly, our findings also showed that a random forest classifier trained on whole-brain qT1 and qT2 surface maps from MRI-positive patients and controls could classify data from MRI-negative patients and controls not used in the training phase. This in turn suggests that there may be an imaging endophenotype of focal epilepsy that is common to MRI-positive and MRI-negative cases.

4.1. qT1 and qT2 changes are unrelated to focus area or focus laterality, and are not driven by FCDs

Importantly, our findings indicate that qT1 and qT2 alterations are likely unrelated to the epileptic focus. Accordingly, though stronger changes were detected in the temporal lobe of TLE patients, such alterations also extended beyond the temporal lobe in this patient sub-group, affecting frontal, occipital and parietal lobes. Such widespread effects were particularly evident when looking at qT1 and qT2 gradients. While no alterations were detected in the sub-group of patients with frontal focus, this is most likely because of the smaller size of this subgroup.

As depth-wise qT1 increases seemed to mostly concern the left hemisphere in patients with left focus, it might be suggested that qT1 increases are related to focus laterality. Importantly, a previous study on patients with TLE (Bernhardt et al., 2018) also demonstrated a strictly ipsilateral distribution of cortical qT1 increases. Notably, in this same study, supervised statistical learning applied to qT1 maps could lateralize the seizure focus in 92% of patients, lending further support to the idea that increases in this metric may be related to the hemispheric focus.

Asymmetry in qT1 depth-wise changes may be due to greater vulnerability of the left hemisphere to early injury and the progressive effects of seizures (Kemmotsu et al., 2011) or a combination of architectural, connectivity, physiological and developmental differences between the hemispheres (Keller et al., 2012) This suggestion is consistent with previous evidence that left-onset patients have much more lateralizing and more significant abnormalities in diffusion measures than right-onset patients (Keller et al., 2012; Kemmotsu et al., 2011; Khan et al., 2014; Shon et al., 2010). This evidence may also explain why, in this study, we failed to detect significant alterations in patients with right hemispheric focus.

However, it is most likely that the smaller sample size of patients with right focus impacted statistical power to detect alterations. Accordingly, gradient maps may constitute a more sensitive approach for picking up such changes. Consistent with this, in contrast to depth-wise qT1 group differences, we detected widespread group effects on qT1 gradient variation across cortical depths, therefore suggesting the presence of bilateral cortical microstructural changes in patients, independent of the side of the seizure focus.

Consistent with the suggestion that microstructural alterations in focal epilepsy are widespread across the cortex and independent of seizure onset or focus laterality, are the extensive qT2 increases detected in the present study, both depth-wise and when looking at the gradient of change in this measure. These findings lend support to previous evidence from TLE, which demonstrates the presence of morphological alterations following a bilateral pattern and extent that is relatively independent of the side of seizure focus (L. Liu et al., 2016). Moreover, our results are very much consistent with a recent study by Ahmad et al. (Ahmad et al., 2020), which employed a surface-based qT2 approach to investigate normal-appearing cortical tissue in adult epilepsy patients with FCDs. Specifically, this study demonstrated widespread cortical qT2 increases in frontal, parietal, and some temporal regions in patients. Additionally, cortical qT2 values in their patient group did not differ between the hemisphere where the FCD was located and the contralateral side.

Altogether, the above evidence supports a global character of cortical changes in focal epilepsy, and suggests the presence of microstructural changes in cortical regions extending beyond FCDs. Accordingly, in this study the detected alterations were not specific to (or driven by) the focal cortical lesions of patients, as demonstrated by the observed heterogeneity of qMRI profiles within the investigated FCDs. Interestingly, the detected heterogeneity of qMRI cortical signatures in patients' lesions supports previous evidence that qMRI changes may be specific to different FCD subtypes (Lorio et al., 2020, 2021).

4.2. qT1 and qT2 changes may reflect myelin disturbance, gliosis, tissue damage, alterations in free-water or a combination of these

There are several underlying microstructural changes that could explain cortical qT1 and qT2 alterations observed in patients in this study. With regards to qT1, previous evidence suggests that this measure may be sensitive to GM myelin content, with lower qT1 values reflecting higher myelination; this is possibly due to myelin cholesterol contributing to longitudinal relaxation times (Hogan, 2017), with studies demonstrating co-occurrence of local changes in intracortical qT1 with the presence of (?) architectonic boundaries (Dick et al., 2012; Lutti et al., 2014; Waehnert et al., 2016). Therefore, increased qT1 values may reflect the presence of cortical myelin disturbance in paediatric focal epilepsy. Consistent with this suggestion, a pathology study of TLE surgical specimens reported alterations in intracortical myelination and fiber arrangement, particularly in upper cortical layers (Thom et al., 2001).

On the other hand, the qT2 increases observed in this study might be explained in terms of gliosis. Previous evidence has reported a correlation between gliosis and hippocampal subfields qT2 in TLE (Peixoto-Santos et al., 2017). Therefore, gliosis on a microstructural level may reflect a remodelling process which might explain the observed qT2 increases (Ahmad et al., 2020). Alternatively, since qT2 is dependent on the free water content in tissue (Cercignani et al., 2018; Deoni et al., 2008), tissue damage and replacement of cells in nervous tissue by water could potentially be another mechanism leading to the increased cortical qT2 values observed in patients.

4.3. qT1 and qT2 alterations may reflect developmental cortical abnormalities in focal epilepsy

Overall, it is uncertain which aetiological factors may be driving these microstructural alterations, whether they represent antecedent neurobiological changes (Widjaja et al., 2012) such as extended aberrant cortico-genesis, or whether they may be a consequence of medication-induced neurotoxicity (De Marcos et al., 2003; Latour et al., 2004) and/or disease processes impacting the cortex over time.

It is possible that seizure activity underlies the qT2 changes observed in this study, as evidence shows that seizures might contribute to gliosis in the hippocampus of patients with TLE (Walker, 2015), and gliosis is associated with qT2 increases (Peixoto-Santos et al., 2017). However, both in our study and previous investigations (Ahmad et al., 2020; R. S. Liu et al., 2003), no significant relationship between structural parameters and seizure occurrence was observed. Additionally, in this study we did not detect an association between qT2 changes and disease duration nor age of onset, and previous evidence reported the lack of an association between the number of anticonvulsive drugs in the medical history and qT2 variation (Ahmad et al., 2020). Overall, the above findings suggest that qT2 alterations may be independent of disease progression and might instead constitute antecedent microstructural alterations reflecting developmental cortical abnormalities.

Though there is not much previous evidence with regards to cortical qT1 relaxometry changes in epilepsy, Bernhardt et al. (2018) showed that increased qT1 within medial temporal and orbital frontal cortices in TLE epilepsy patients was associated with age of epilepsy onset, thus suggesting these alterations may reflect atypical neurodevelopment (Bernhardt et al., 2018). In accord with this suggestion, an earlier pathology report on TLE specimens noted subtle architectural anomalies of intracortical myelination and fiber arrangement, particularly in upper cortical layers (Thom et al., 2001).

Consistent with qT1 and qT2 abnormalities reflecting antecedent anomalies in brain development, a longitudinal study of children with new-onset epilepsy demonstrated differences in baseline GM and WM volumes of patients compared to controls (Tosun et al., 2011). Additionally, the authors also reported slowed WM expansions and changes in GM volume in patients at 2-year follow up. Again providing support for the presence of antecedent cortical anomalies in epilepsy, Widjaja and colleagues reported changes in cortical thickness in the right medial temporal, cingulate, and left frontal cortices in children with new-onset seizures (Widjaja et al., 2012). Importantly, it is possible that such antecedent brain changes may predispose patients to seizures, although this hypothesis requires further investigation.

Finally, though the relation of qT1 and qT2 abnormalities to epileptogenicity remains uncertain, in the present study, qT1 and qT2 relaxometry changes did not appear specific to the focal cortical lesion, suggesting that children with drug-resistant focal epilepsy may present a diffuse abnormality of the structure of the brain despite the focal nature of the visualised lesions. This in turn implies that visible FCDs may simply constitute the most apparent manifestation of abnormal structure in an extensively disorganized brain (Sisodiya et al., 1995).

4.4. qMRI as a possible new approach to the classification of MRI-negative children with drug resistant focal epilepsy

In this study, we provide preliminary results that global cortical changes in surface-based qT1 and qT2 can classify children with drug-resistant focal epilepsy. This suggests the presence of a potential imaging endophenotype of focal epilepsy, detectable with or without radiologically identified abnormalities being present. Crucially, its ability to classify young patients may suggest that such endophenotype may be present at a pre-symptomatic disease stage.

4.5. Conclusion

Widespread, rather than focal, depth-mediated qT1 and qT2 increases were demonstrated in the cortex of children with treatment-resistant focal epilepsy. Such changes likely represent loss of structure such as altered cortical stratification, gliosis, myelin and iron changes, oedema-associated increase in free-water (Cercignani et al., 2018), or combination of these.

Though the aetiology of these cortical alterations is not fully understood, it is possible that such microstructural changes appear during cerebral development and represent precedent neurobiological alterations, rather than the cumulative effect of recurrent seizures or the consequence of medications' side-effects. Accordingly, based on our findings it is plausible to suggest that global cortical changes in surface-based qT1 and qT2 may constitute a potential imaging endophenotype of focal epilepsy, detectable with or without the presence of radiologically identified abnormalities and disease-onset. This suggestion is in accord with previous evidence demonstrating structural thalamic abnormalities at the initial onset of genetic generalized epilepsy in antiepileptic drugs-naive patients (Perani et al., 2018).

Further studies evaluating qT1 and qT2 changes and histopathology will be necessary to confirm whether qT1 and qT2 are markers of widespread abnormal cortical development. Importantly, this study was conducted using a cross-sectional design, therefore limiting control over the confounding effect of age. Future relaxometry studies assessing paediatric patients with new-onset seizures longitudinally will enable to better disentangle the impact of age from the effect of disease, as well as of recurrent seizures and long-term antiepileptic medications on the brain. The specificity of these global cortical changes to focal epilepsy as opposed to seizures is unclear and inclusion of other epilepsies is needed.

Additionally, future investigations could provide complementary information to the existing evidence by assessing cortical alterations in T2* and quantitative susceptibility, diffusion-based microstructural and connectivity changes, as well as the association of such changes with disease duration.

Most importantly, approaches that address patients heterogeneity, such as normative modelling (Marquand et al., 2016), will allow to control for brain variability and rapid, non-linear tissue changes associated with development (Norbom et al., 2021), and therefore to better disentangle significant pathologic changes from 'normal' or expected age-related alterations.

Acknowledgements:
We are grateful to the families who generously supported this study. We also thank the Pediatric Neurology team from the Evelina London Children Hospital, including Dr. Ruth Williams, Dr. Elaine Hughes, Dr. Shan Tang, and Dr. Karine Lascelles.

Funding:
The study was funded by a Sir Henry Dale Fellowship jointly funded by the Wellcome Trust and the Royal Society (206675/Z/17/Z). This research was also supported by GOSHCC Sparks Grant V4419, King's Health Partners, in part by the Medical Research Council (UK) (grants MR/K006355/1 and MR/LO11530/1) and Medical Research Council Center for Neurodevelopmental Disorders, King's College London (MR/N026063/1), and by core funding from the Wellcome Engineering and Physical Sciences Research Council Centre for Medical Engineering at King's College London [WT203148/Z/16/Z]. Infrastructure support was provided by the National Institute for Health Research Mental Health Biomedical Research Centre at South London, Maudsley NHS Foundation Trust, King's College London and the National Institute for Health Research Mental Health Biomedical Research Centre at Guy's and St Thomas' Hospitals NHS Foundation Trust.

References

Adler, S., Hong, S., Liu, M., Baldeweg, T., Cross, J. H., Bernasconi, A., Bernhardt, B. C., & Bernasconi, N. (2018). Topographic principles of cortical fluid-attenuated inversion recovery signal in temporal lobe epilepsy. *Epilepsia*, *59*(3), 627–635.

Adler, S., Lorio, S., Jacques, T. S., Benova, B., Gunny, R., Cross, J. H., Baldeweg, T., & Carmichael, D. W. (2017). Towards in vivo focal cortical dysplasia phenotyping using quantitative MRI. *NeuroImage : Clinical*, *15*, 95–105.

Ahmad, R., Maiworm, M., Nöth, U., Seiler, A., Hattingen, E., Steinmetz, H., Rosenow, F., Deichmann, R., Wagner, M., & Gracien, R.-M. (2020). Cortical Changes in Epilepsy Patients With Focal Cortical Dysplasia: New Insights With T2 Mapping. *Journal of Magnetic Resonance Imaging*, *52*(6), 1783–1789.

Annese, J., Pitiot, A., Dinov, I. D., & Toga, A. W. (2004). A myelo-architectonic method for the structural classification of cortical areas. *NeuroImage*, *21*(1), 15–26.

Bernhardt, B. C., Fadaie, F., de Wael, R. V., Hong, S.-J., Liu, M., Guiot, M. C., Rudko, D. A., Bernasconi, A., & Bernasconi, N. (2018). Preferential susceptibility of limbic cortices to microstructural damage in temporal lobe epilepsy: A quantitative T1 mapping study. *Neuroimage*, *182*, 294–303.

Breiman, L. (2001). Random Forests. *Machine Learning*, *45*(1), 5–32.

Caciagli, L., Bernasconi, A., Wiebe, S., Koepp, M. J., Bernasconi, N., & Bernhardt, B. C. (2017). A meta-analysis on progressive atrophy in intractable temporal lobe epilepsy: Time is brain? *Neurology*, *89*(5), 506–516.

Cercignani, M., Dowell, N. G., & Tofts, P. S. (2018). *Quantitative MRI of the Brain: Principles of Physical Measurement, Second edition*. CRC Press.

Cordero-Grande, L., Ferrazzi, G., Teixeira, R. P. A., O'Muircheartaigh, J., Price, A. N., & Hajnal, J. V. (2020). Motion-corrected MRI with DISORDER: Distributed and incoherent sample orders for reconstruction deblurring using encoding redundancy. *Magnetic Resonance in Medicine*, *84*(2), 713–726.

Cordero-Grande, L., Teixeira, R. P. A., Hughes, E. J., Hutter, J., Price, A. N., & Hajnal, J. V. (2016). Sensitivity encoding for aligned multishot magnetic resonance reconstruction. *IEEE Transactions on Computational Imaging*, *2*(3), 266–280.

De Marcos, F. A., Ghizoni, E., Kobayashi, E., Li, L. M., & Cendes, F. (2003). Cerebellar volume and long-term use of phenytoin. *Seizure*, *12*(5), 312–315.

Deoni, S. C., Rutt, B. K., Arun, T., Pierpaoli, C., & Jones, D. K. (2008). Gleaning multicomponent T1 and T2 information from steady-state imaging data. *Magnetic Resonance in Medicine: An Official Journal of the International Society for Magnetic Resonance in Medicine*, *60*(6), 1372–1387.

Dick, F., Tierney, A. T., Lutti, A., Josephs, O., Sereno, M. I., & Weiskopf, N. (2012). In vivo functional and myeloarchitectonic mapping of human primary auditory areas. *Journal of Neuroscience*, *32*(46), 16095–16105.

Donaire, A., Carreno, M., Gomez, B., Fossas, P., Bargalló, N., Agudo, R., Falip, M., Setoaín, X., Boget, T., & Raspall, T. (2006). Cortical laminar necrosis related to prolonged focal status epilepticus. *Journal of Neurology, Neurosurgery & Psychiatry*, *77*(1), 104–106.

Fauser, S., Schulze-Bonhage, A., Honegger, J., Carmona, H., Huppertz, H.-J., Pantazis, G., Rona, S., Bast, T., Strobl, K., & Steinhoff, B. J. (2004). Focal cortical dysplasias: Surgical outcome in 67 patients in relation to histological subtypes and dual pathology. *Brain*, *127*(11), 2406–2418.

Galovic, M., de Tisi, J., McEvoy, A. W., Miserocchi, A., Vos, S. B., Borzi, G., Cueva Rosillo, J., Vuong, K. A., Nachev, P., & Duncan, J. S. (2020). Resective surgery prevents progressive cortical thinning in temporal lobe epilepsy. *Brain*, *143*(11), 3262–3272.

Glasser, M. F., Sotiropoulos, S. N., Wilson, J. A., Coalson, T. S., Fischl, B., Andersson, J. L., Xu, J., Jbabdi, S., Webster, M., Polimeni, J. R., Van Essen, D. C., Jenkinson, M., & WU-Minn HCP Consortium. (2013). The minimal preprocessing pipelines for the Human Connectome Project. *NeuroImage*, *80*, 105–124.

Hattingen, E., Enkirch, S. J., Jurcoane, A., Kruse, M., Delev, D., Grote, A., & Becker, A. (2018). Hippocampal "gliosis only" on MR imaging represents a distinct entity in epilepsy patients. *Neuroradiology*, *60*(2), 161–168.

Hogan, R. E. (2017). Quantitative Measurement of Longitudinal Relaxation Time (qT1) Mapping in TLE: A Marker for Intracortical Microstructure? *Epilepsy Currents*, *17*(6), 358–360.

Keller, S. S., Schoene-Bake, J.-C., Gerdes, J. S., Weber, B., & Deppe, M. (2012). Concomitant fractional anisotropy and volumetric abnormalities in temporal lobe epilepsy: Cross-sectional evidence for progressive neurologic injury. *PloS One*, *7*(10), e46791.

Kemmotsu, N., Girard, H. M., Bernhardt, B. C., Bonilha, L., Lin, J. J., Tecoma, E. S., Iragui, V. J., Hagler Jr, D. J., Halgren, E., & McDonald, C. R. (2011). MRI analysis in temporal lobe epilepsy: Cortical thinning and white matter disruptions are related to side of seizure onset. *Epilepsia*, *52*(12), 2257–2266.

Khan, A. R., Goubran, M., de Ribaupierre, S., Hammond, R. R., Burneo, J. G., Parrent, A. G., & Peters, T. M. (2014). Quantitative relaxometry and diffusion MRI for lateralization in MTS and non-MTS temporal lobe epilepsy. *Epilepsy Research*, *108*(3), 506–516.

Latour, P., Biraben, A., Polard, E., Bentué-Ferrer, D., Beauplet, A., Tribut, O., & Allain, H. (2004). Drug induced encephalopathy in six epileptic patients: Topiramate? valproate? or both? *Human Psychopharmacology*, *19*(3), 193–203.

Liu, L., Bernhardt, B. C., Bernasconi, A., & Bernasconi, N. (2016). Gray matter structural compromise is equally distributed in left and right temporal lobe epilepsy. *Human Brain Mapping*, *37*(2), 515–524.

Liu, R. S., Lemieux, L., Bell, G. S., Hammers, A., Sisodiya, S. M., Bartlett, P. A., Shorvon, S. D., Sander, J. W., & Duncan, J. S. (2003). Progressive neocortical damage in epilepsy. *Annals of Neurology: Official Journal of the American Neurological Association and the Child Neurology Society*, *53*(3), 312–324.

Lorio, S., Adler, S., Gunny, R., D'Arco, F., Kaden, E., Wagstyl, K., Jacques, T. S., Clark, C. A., Cross, J. H., Baldeweg, T., & Carmichael, D. W. (2020). MRI profiling of focal cortical dysplasia using multi-compartment diffusion models. *Epilepsia*, *61*(3), 433–444.

Lorio, S., Sedlacik, J., So, P.-W., Parkes, H. G., Gunny, R., Löbel, U., Li, Y.-F., Ogunbiyi, O., Mistry, T., Dixon, E., Adler, S., Cross, J. H., Baldeweg, T., Jacques, T. S., Shmueli, K., & Carmichael, D. W. (2021). Quantitative MRI susceptibility mapping reveals cortical signatures of changes in iron, calcium and zinc in malformations of cortical development in children with drug-resistant epilepsy. *NeuroImage*, *238*, 118102.

Lutti, A., Dick, F., Sereno, M. I., & Weiskopf, N. (2014). Using high-resolution quantitative mapping of R1 as an index of cortical myelination. *Neuroimage*, *93*, 176–188.

Marquand, A. F., Rezek, I., Buitelaar, J., & Beckmann, C. F. (2016). Understanding Heterogeneity in Clinical Cohorts Using Normative Models: Beyond Case-Control Studies. *Biological Psychiatry*, *80*(7), 552–561.

Norbom, L. B., Ferschmann, L., Parker, N., Agartz, I., Andreassen, O. A., Paus, T., Westlye, L. T., & Tamnes, C. K. (2021). New insights into the dynamic development of the cerebral cortex in childhood and adolescence: Integrating macro- and microstructural MRI findings. *Progress in Neurobiology*, *204*, 102109.

Pedregosa, F., Varoquaux, G., Gramfort, A., Michel, V., Thirion, B., Grisel, O., Blondel, M., Prettenhofer, P., Weiss, R., & Dubourg, V. (2011). Scikit-learn: Machine learning in Python. *The Journal of Machine Learning Research*, *12*, 2825–2830.

Peixoto-Santos, J. E., Kandratavicius, L., Velasco, T. R., Assirati, J. A., Carlotti, C. G., Scandiuzzi, R. C., Salmon, C. E. G., Santos, A. C. D., & Leite, J. P. (2017). Individual hippocampal subfield assessment indicates that matrix macromolecules and gliosis are key elements for the increased T2 relaxation time seen in temporal lobe epilepsy. *Epilepsia*, *58*(1), 149–159.

Perani, S., Tierney, T. M., Centeno, M., Shamshiri, E. A., Yaakub, S. N., O'Muircheartaigh, J., Carmichael, D. W., & Richardson, M. P. (2018). Thalamic volume reduction in drug-naive patients with new-onset genetic generalized epilepsy. *Epilepsia*, *59*(1), 226–234.

Shon, Y., Kim, Y., Koo, B., Lee, J., Kim, H. J., Kim, W. J., Ahn, K. J., & Yang, D. W. (2010). Group-specific regional white matter abnormality revealed in diffusion tensor imaging of medial temporal lobe epilepsy without hippocampal sclerosis. *Epilepsia*, *51*(4), 529–535.

Sisodiya, S., Free, S., Stevens, J., Fish, D., & Shorvon, S. (1995). Widespread cerebral structural changes in patients with cortical dysgenesis and epilepsy. *Brain*, *118*(4), 1039–1050.

Smith, S. M., & Nichols, T. E. (2009). Threshold-free cluster enhancement: Addressing problems of smoothing, threshold dependence and localisation in cluster inference. *NeuroImage*, *44*(1), 83–98.

Teixeira, R. P. A. G., Malik, S. J., & Hajnal, J. V. (2018). Joint system relaxometry (JSR) and Crámer-Rao lower bound optimization of sequence parameters: A framework for enhanced precision of DESPOT T1 and T2 estimation. *Magnetic Resonance in Medicine*, *79*(1), 234–245.

Thom, M., Sisodiya, S., Harkness, W., & Scaravilli, F. (2001). Microdysgenesis in temporal lobe epilepsy: A quantitative and immunohistochemical study of white matter neurones. *Brain*, *124*(11), 2299–2309.

Tosun, D., Dabbs, K., Caplan, R., Siddarth, P., Toga, A., Seidenberg, M., & Hermann, B. (2011). Deformation-based morphometry of prospective neurodevelopmental changes in new onset paediatric epilepsy. *Brain*, *134*(4), 1003–1014.

Vecchiato, K., Egloff, A., Carney, O., Siddiqui, A., Hughes, E., Dillon, L., Colford, K., Green, E., Texeira, R. P. a. G., Price, A. N., Ferrazzi, G., Hajnal, J. V., Carmichael, D. W., Cordero-Grande, L., & O'Muircheartaigh, J. (2021). Evaluation of DISORDER: Retrospective Image Motion Correction for Volumetric Brain MRI in a Pediatric Setting. *American Journal of Neuroradiology*, *42*(4), 774–781.

Waehnert, M. D., Dinse, J., Schäfer, A., Geyer, S., Bazin, P.-L., Turner, R., & Tardif, C. L. (2016). A subject-specific framework for in vivo myeloarchitectonic analysis using high resolution quantitative MRI. *Neuroimage*, *125*, 94–107.

Walker, M. C. (2015). Hippocampal Sclerosis: Causes and Prevention. *Seminars in Neurology*, *35*(3), 193–200.

Widjaja, E., Zarei Mahmoodabadi, S., Go, C., Raybaud, C., Chuang, S., Snead, O. C., & Smith, M. L. (2012). Reduced Cortical Thickness in Children with New-Onset Seizures. *AJNR: American Journal of Neuroradiology*, *33*(4), 673–677.

Winkler, A. M., Greve, D. N., Bjuland, K. J., Nichols, T. E., Sabuncu, M. R., Håberg, A. K., Skranes, J., & Rimol, L. M. (2018). Joint Analysis of Cortical Area and Thickness as a Replacement for the Analysis of the Volume of the Cerebral Cortex. *Cerebral Cortex (New York, NY)*, *28*(2), 738–749.

Winkler, A. M., Ridgway, G. R., Webster, M. A., Smith, S. M., & Nichols, T. E. (2014). Permutation inference for the general linear model. *NeuroImage*, *92*, 381–397.

Winkler, A. M., Webster, M. A., Brooks, J. C., Tracey, I., Smith, S. M., & Nichols, T. E. (2016). Non-parametric combination and related permutation tests for neuroimaging. *Human Brain Mapping*, *37*(4), 1486–1511.

Woermann, F. G., Free, S. L., Koepp, M. J., Ashburner, J., & Duncan, J. S. (1999). Voxel-by-voxel comparison of automatically segmented cerebral gray matter—A rater-independent comparison of structural MRI in patients with epilepsy. *Neuroimage*, *10*(4), 373–384.

Wood, T. C. (2018). QUIT: QUantitative Imaging Tools. *Journal of Open Source Software*, *3*(26), 656.